Histomorphometry and Bone Mechanical Property Evolution Around Different Implant Systems at Early Healing Stages: An Experimental Study in Dogs

Ryo Jimbo, DDS, PhD,* Rodolfo Anchieta, DDS, MS,† Marta Baldassarri, PhD,† Rodrigo Granato, DDS, MS, PhD,‡ Charles Marin, DDS, MS,§ Hellen S. Teixeira, DDS,‖ Nick Tovar, PhD,¶ Stefan Vandeweghe, DDS, PhD,# Malvin N. Janal, PhD,** and Paulo G. Coelho, DDS, PhD††

Majority of the commercially available implants on the market today is a combination of optimal implant properties in the macro-, micro-, and nanometer levels. These circumstantial designs are based on the extensive and scrupulous investigations both from the theoretical and practical aspects,[1–4] and various factors such as topography, chemistry, and surface energy/hydrophilicity have been considered during this process. For instance, it has been indicated that surface blasting techniques may provide a completely different surface topography depending on the particle size, velocity, and the

Purpose: Commercial implants differ at macro-, micro-, and nano-levels, which makes it difficult to distinguish their effect on osseointegration. The aim of this study was to evaluate the early integration of 5 commercially available implants (Astra OsseoSpeed, Straumann SLA, Intra-Lock Blossom Ossean, Nobel Active, and OsseoFix) by histomorphometry and nanoindentation.

Materials and Methods: Implants were installed in the tibiae of 18 beagle dogs. Samples were retrieved at 1, 3, and 6 weeks (n = 6 for each time point) and were histologically and nanomechanically evaluated.

Results: The results presented that both time (P < 0.01) and implant system and time interaction (P < 0.02) significantly affected the bone-to-implant contact (BIC). At 1 week, the different groups presented statistically different outcomes. No significant changes in BIC were noted thereafter. There were no significant differences in rank elastic modulus (E) or in rank hardness (H) for time (E: P > 0.80; H: P > 0.75) or implant system (E: P > 0.90; H: P > 0.85).

Conclusions: The effect of different implant designs on osseointegration was evident especially at early stages of bone healing. (Implant Dent 2013;0:1–8)

Key Words: nanoindentation, osseointegration, histology

*Associate Professor, Department of Prosthodontics, Faculty of Odontology, Malmö University, Malmö, Sweden.
†Researcher, Department of Biomaterials and Biomimetics, New York University College of Dentistry, New York, NY; Private Practice, Paris, France.
‡Lecturer, Department of Dentistry, Universidade Federal de Santa Catarina, Florianopolis, Brazil.
§Assistant Professor, Department of Dentistry, UNIGRANRIO, Duque de Caxias, Rio de Janeiro, Brazil.
‖Researcher, Department of Biomaterials and Biomimetics, New York University College of Dentistry, New York, NY.
¶Adjunct Professor, Department of Biomaterials and Biomimetics, New York University College of Dentistry, New York, NY.
#Assistant Professor, Department of Periodontology and Oral Implantology, Dental School, Faculty of Medicine and Health Sciences, University of Ghent, Belgium.
**Senior Research Scientist, Department of Epidemiology, New York University College of Dentistry, New York, NY.
††Assistant Professor of Biomaterials and Biomimetics and Director for Research, Department of Periodontology and Implant Dentistry, New York University College of Dentistry, New York, NY.

Reprint requests and correspondence to: Ryo Jimbo, DDS, PhD, Department of Prosthodontics, Faculty of Odontology, Malmö University, Malmö 205 06, Sweden, Phone: +46 40 665 8679, Fax: + 46 40 665 8503, E-mail: ryo.jimbo@mah.se

surface coverage,[5] and it has been proven that there is an optimal surface microtopography that presents potent biologic response.[6] Furthermore, characterization of implant surface chemistry and surface hydrophilicity has been suggested to be a decisive factor for the enhancement of osseointegration, because the slight modification of these variables results in different biologic outcomes.[7–11] Paradoxically, the combination of multiple variables has made the implant design complex and has

made it difficult to distinguish from one implant to another. In fact, the time to osseointegrated has significantly enhanced with the so-called modern implants, and the long-term success including the marginal bone stability has been reported to be analogous with most of the available commercial implants existing today.[12] This is one of the reasons why the outcomes of the commercially available implants are thought to be, in general, similar especially among clinicians.

In accordance with the clinical outcomes, it is indeed a fact that, even for *in vivo* animal studies, the differences between various modifications are extremely difficult to capture, especially with the conventional techniques such as histology or biomechanics. However, when exploring the covariance or the correlation among different conventional variables using the principle component analysis, it was statistically evident that variables such as bone-to-implant contact (BIC), bone area, mineralization rate, implant resonance frequency, or removal torque were independently correlated to different implant modifications, suggesting that different implants, in fact, do respond to biology in a unique manner.[13,14]

To further distinguish the characteristics of different implant modifications, novel approaches have been proposed and have proven to be effective. In a clinically related simulation study, a computer tomography-based finite element analysis has successfully simulated and clarified the differences between different implant designs in immediately placed situations and, additionally, provided some clinical implications.[15] In animal studies, it has been reported that using 3-dimensional approaches, such as the microcomputed tomography, or evaluation of the genetic expression using the real-time polymerase chain reaction has revealed the detailed characteristics of the different implant designs in the microscopic and molecular levels.[16–19]

The commonly used method to determine the degree of osseointegration is the BIC. It has been extensively proven in a number of *in vivo* animal studies that the modern oral implants regenerate bone faster than their predecessors in terms of the BIC.[7,20–23] From a clinical perspective, it would be further beneficial to evaluate the bone nanomechanical properties of the contacting bone to different implants, because this could provide additional information regarding the quality of the bone, and this may possibly be correlative to the so-called implant secondary (biologic) stability. Thus, the aim of this *in vivo*

animal study is to evaluate the osteoconductivity of 5 different commercially available implants histomorphometrically and further to evaluate the bone nanomechanical properties using the nanoindentation technique.

MATERIALS AND METHODS

Animals and Implantation

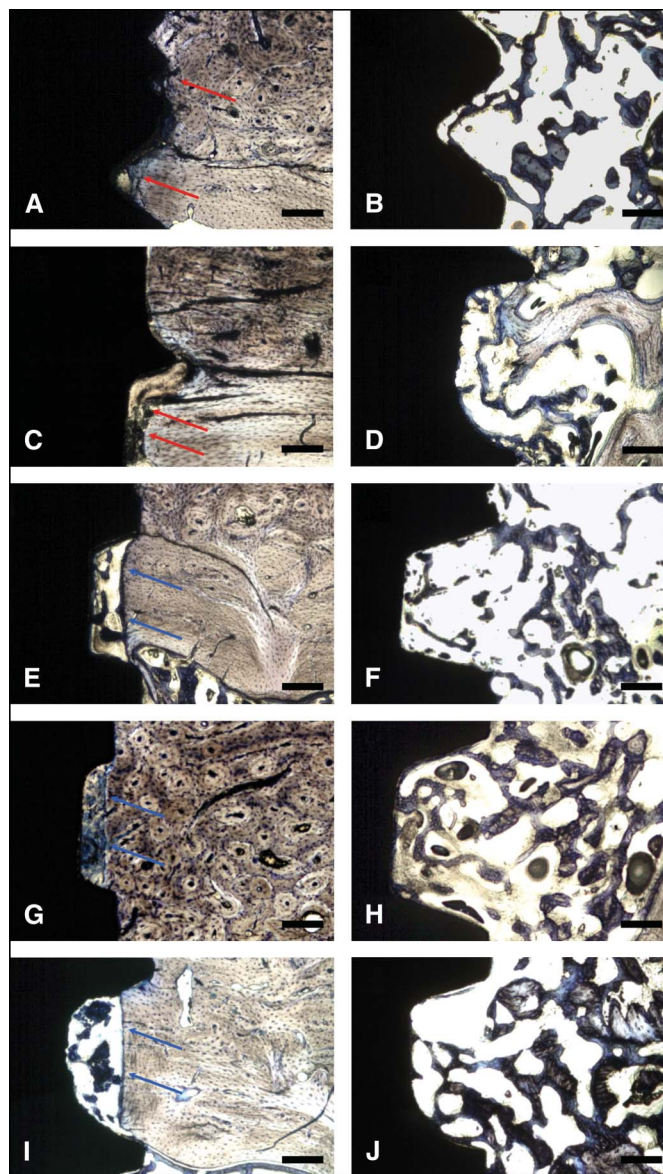Eighteen adult beagle dogs aged 1.5 years were used for the study. The experimental protocol has been approved

Fig. 1. One-week *in vivo* optical micrographs of Astra OsseoSpeed at (**A**) cortical region and (**B**) trabecular regions, of Straumann SLA at (**C**) cortical region and (**D**) trabecular regions, of Nobel Active at (**E**) cortical region and (**F**) trabecular regions, of Adin OsseoFix at (**G**) cortical region and (**H**) trabecular regions, and of IL Ossean at (**I**) cortical region and (**J**) trabecular regions. In regions of cortical bone, initial interface remodeling was observed at the regions where direct engagement between the implant and bone existed at the cortical immediately after placement (Astra OsseoSpeed implant microthread regions and the Straumann SLA cervical third, red arrows in **A** and **C**). For the other 3 systems, the interplay between the implant bulk design and drilling dimensions allowed for empty spaces (healing chambers, denoted by blue arrows in **E**, **G**, and **I**) of different dimensions bounded by the implant surface and cortical bone, which, at 1 week, presented initial woven bone formation. In regions of trabecular bone, initial formation of woven bone was observed in direct contact or in proximity of all implant surfaces (**B**, **D**, **F**, **H**, and **J**). Bars represent 100 μm.
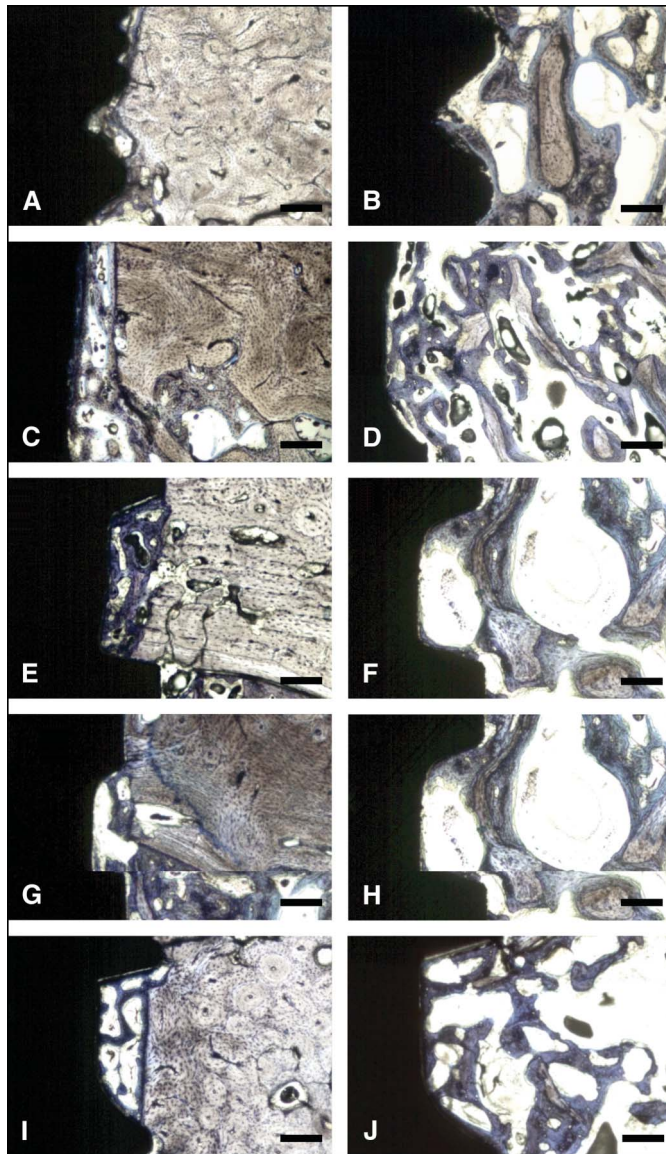
Fig. 2. Three weeks *in vivo* optical micrographs of Astra OsseoSpeed at (**A**) cortical region and (**B**) trabecular regions, of Straumann SLA at (**C**) cortical region and (**D**) trabecular regions, of Nobel Active at (**E**) cortical region and (**F**) trabecular regions, of Adin OsseoFix at (**G**) cortical region and (**H**) trabecular regions, and of IL Ossean at (**I**) cortical region and (**J**) trabecular regions. In regions of cortical bone where primary engagement occurred immediately after implant placement, interfacial remodeling resulted in a newly formed bone filling the gap between the cortical bone and implant surface (**A** and **C**). Conversely, implant system that allowed the formation of healing chambers showed higher degree of interaction between the bone and implant surface (**E**, **G**, and **I**). In regions of trabecular bone, the formation of woven bone progressed relative to the 1-week time point either in direct contact or in proximity of all implant surfaces (**B**, **D**, **F**, **H**, and **J**). In these regions, initial woven bone remodeling sites were seldom observed. Bars represent 100 μm.

Straumann SLA (Straumann, Basel, Switzerland), Intra-Lock Blossom Ossean (Intralock International, Boca Raton, FL), Nobel Active (Nobel Biocare, Balsberg, Switzerland), and Osseo-Fix (Adin, Galilee, Israel). The implants were randomly placed starting from approximately 2 cm below the joint capsule line at the central anteromedial position of the proximal tibiae down. The other 4 implants were placed along the distal direction at distances of approximately 1 cm from each other along the central region of the bone. All implants were placed according to the suggested procedures provided by each manufacturer. Thereafter, the soft tissue was sutured in layers, where the periosteum was sutured with Vicryl 4-0 (Ethicon Johnson, Miami, FL) and the skin with 4-0 nylon (Ethicon Johnson). Postoperatively, animals were given a single dose of benzyl penicillin benzatine (20,000 UI/kg) and Ketoprofen (1%; 1 mL/5 kg, intramuscularly). The animals were killed after 1 week (n = 6), 3 weeks (n = 6), and 6 weeks (n = 6) with an overdose of anesthesia.

Histologic Sectioning and Histomorphometry

At each time point, the samples were retrieved *en bloc* and placed in 10% formaldehyde for 24 hours, thereafter were subjected to a series of dehydration and infiltration procedures; finally, the samples were embedded in a methacrylate-based resin (Technovit 9100; Heraeus Kulzer GmbH, Wehrheim, Germany) according to the manufacturer's instructions. After polymerization, the embedded samples were cut at the center of the implant along its long axis with a diamond saw (Isomet 2000; Buehler, Ltd., Lake Bluff, IL), were subjected to grinding and polishing using a series of SiC abrasive papers to a final thickness of approximately 30 μm, and were then toluidine blue stained; finally, the sections were histomorphologically evaluated under light optical microscope. The BIC was determined using an optical microscope (Leica DM2500M; Leica Microsystems GmbH, Wetzlar, Germany), and the captured images were further analyzed using a computer software (Leica Application Suite; Leica Microsystems GmbH).

by the Ecole Nationale Veterinaire d'Alfort. All surgeries were conducted under general inhalation anesthesia.

The tibia on 1 leg was used for the study. The surgical sites were initially shaved and were disinfected with antiseptic iodine solution. After incision and elevation of the periosteum, osteotomies were made with sequential drills under saline irrigation. Five commercially available implants (all at dimensions of ~4 mm diameter and ~10 mm length) were used in this study: Astra OsseoSpeed (Astra Tech, Mölndal, Sweden),
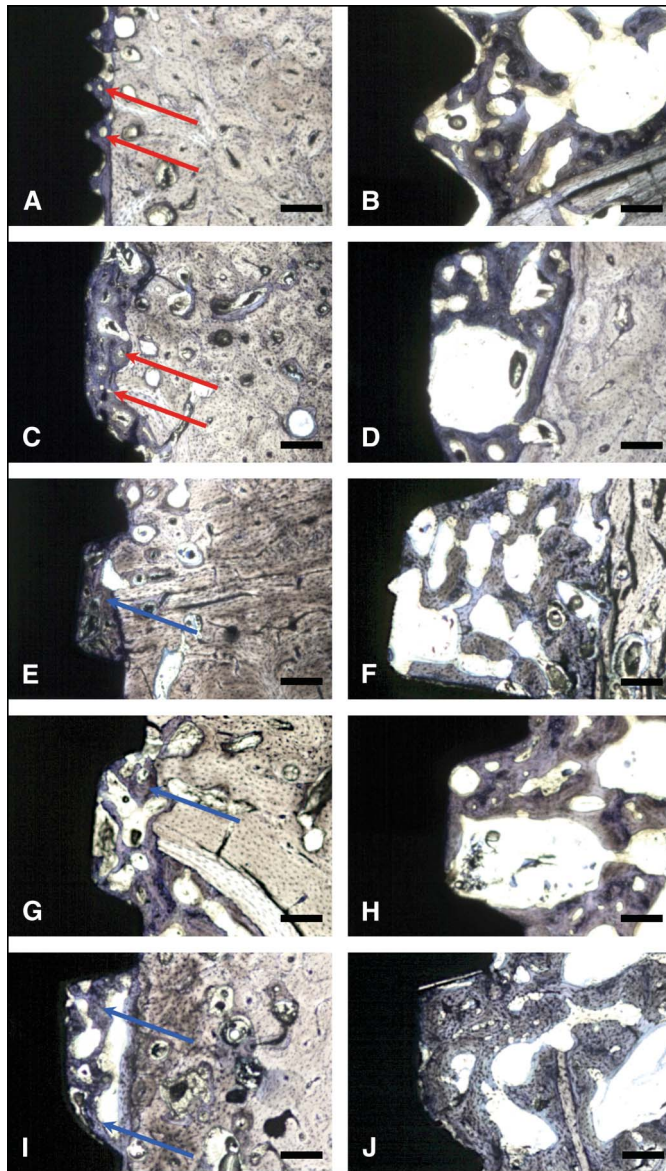
Fig. 3. Six weeks *in vivo* optical micrographs of Astra OsseoSpeed at (**A**) cortical region and (**B**) trabecular regions, of Straumann SLA at (**C**) cortical region and (**D**) trabecular regions, of Nobel Active at (**E**) cortical region and (**F**) trabecular regions, of Adin OsseoFix at (**G**) cortical region and (**H**) trabecular regions, and of IL Ossean at (**I**) cortical region and (**J**) trabecular regions. In regions of cortical bone where primary engagement occurred immediately after implant placement, bone remodeling sites were observed on the woven bone filling the gap between the cortical bone and implant surface (red arrows in **A** and **C**). For the implant systems that allowed the formation of healing chambers, initial replacement of woven bone by lamellar bone was observed (blue arrows on **E**, **G**, and **I**). In regions of trabecular bone, initial replacement of woven bone by lamellar bone was observed irrespective of the implant group (**B**, **D**, **F**, **H**, and **J**). In these regions, multiple bone remodeling sites were observed. Bars represent 100 μm.

Nanoindentation

In total, indentations were performed with an average of 25 indentations per histologic section. A nanoindenter (Hysitron, Minneapolis, MN) equipped with a Berkovich diamond 3-sided pyramid probe was used. Indentations in the same specimen were performed in a newly formed bone to 0.5 mm from the implant surface with a distance of at least 10 μm from each other so that no interactions between them affected the mechanical results.[24] A wax chamber was created above the acrylic plate around the implant-in-bone perimeter, so that tests were performed in water.[25] A loading profile was developed with a peak load of 300 μN at a rate of 60 μN/s, followed by a holding time of 10 seconds and an unloading time of 2 seconds. The extended holding period allowed bone to relax to a more linear response, so that no tissue creep effect was occurring in the unloading portion of the profile (ISO 14577-4). Therefore, from each indentation, a load-displacement curve was obtained.[26]

Bone tissue was detected by imaging under the light microscope (Hysitron TI 950), and the indentations were performed for the 3- and 6-week samples. The nanomechanical testing was performed for the 3- and 6-week samples because samples from first week presented new bone formation limited to a thin layer of bone onto the implant surface at regions of trabecular bone, and the appropriate placement of the Berkovich indenter in such narrow region of new bone formation could not be consistently achieved.

From each analyzed load-displacement curve, reduced modulus (GPa) and hardness (GPa) of bone tissue were computed and its elastic modulus E_b (GPa) was calculated as follows:

$$\frac{1}{E_r} = \frac{1 - V_b^2}{E_b} + \frac{1 - V_i^2}{E_i},$$

where E_r is the reduced modulus (GPa), V_b (0.3) is the Poisson ratio for cortical bone, and E_i (1140 GPa) and V_i (0.07) are the elastic modulus and Poisson ratio for the indenter, respectively.[27–29]

Statistical Analysis

All statistical analyses were performed at a 95% level of significance. Statistical analysis for BIC was performed by GLM ANOVA considering implant type and time *in vivo* as independent variables. For the nanoindentation outcomes, the collected data were ranked and the GLM ANOVA was used to evaluate the effects of implant type and time *in vivo* in both elastic modulus and hardness.

RESULTS

Histologic Observation and Histomorphometry

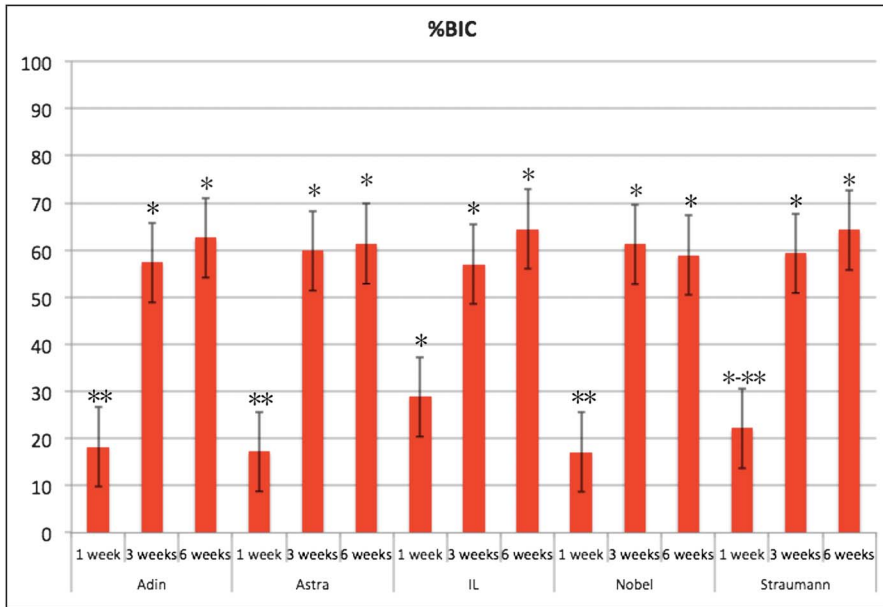The histologic results showed that all implants were integrated with bone

Fig. 4. BIC as a function of implant system and time *in vivo*. Note that the number of asterisks represents statistically homogeneous groups for each individual time *in vivo*.

Fig. 5. Rank elastic modulus as a function of (**A**) time, (**B**) implant system, and (**C**) time and implant system. Note that the number of asterisks depicts statistically homogeneous groups.

and direct contact between the implant and bone occurred at both cortical and trabecular regions. In general, irrespective of the implant group, similar trends were observed at all times *in vivo*, and these were related to how engagement between the implant and bone occurred immediately after insertion.

At 1 week *in vivo*, in regions of cortical bone, initial interface remodeling was observed at the regions where direct engagement between the implant and bone existed (Fig. 1) at the cortical immediately after placement (for the Astra OsseoSpeed, implant microthread regions, and for the Straumann SLA, cervical third). For the other 3 systems, the interplay between the implant bulk design and drilling dimensions allowed for empty spaces (healing chambers) of different dimensions bounded by the implant surface and cortical bone, which, at 1 week, presented initial woven bone formation (Fig. 1, E, G, and I). In regions of trabecular bone, initial woven bone formation was observed in direct contact or in proximity of all implants surfaces (Fig. 1, B, D, F, H, and J).

At 3 weeks, in regions of cortical bone where primary engagement between the implant and the bone occurred immediately after implant placement, interfacial remodeling resulted in the newly formed bone filling the gap

between the cortical bone and implant surface (Fig. 2, A and C). Nevertheless, implant systems that allowed the formation of healing chambers showed higher degree of interaction between the bone and implant surface (Fig. 2, E, G, and I). In regions of trabecular bone, woven bone formation progressed relative to the 1-week time point either in direct contact or in proximity of all implant surfaces (Fig. 2, B, D, F, H, and J). In these regions, initial woven bone remodeling sites were seldom observed.

At 6 weeks, in regions of cortical bone where primary engagement between the implant and the bone occurred immediately after implant placement, bone remodeling sites were observed on the woven bone filling the gap between the cortical bone and implant surface (Fig. 3, A and C). For the implant system that allowed the formation of healing chambers, initial replacement of woven bone by lamellar bone was observed (Fig. 3, E, G, and I). In regions of trabecular bone, initial replacement of woven bone by lamellar bone was observed irrespective of the implant group (Fig. 3, B, D, F, H, and J). In these regions, multiple bone remodeling sites were observed.

The BIC results showed that both time ($P < 0.01$) and implant system and time ($P < 0.02$) interaction significantly
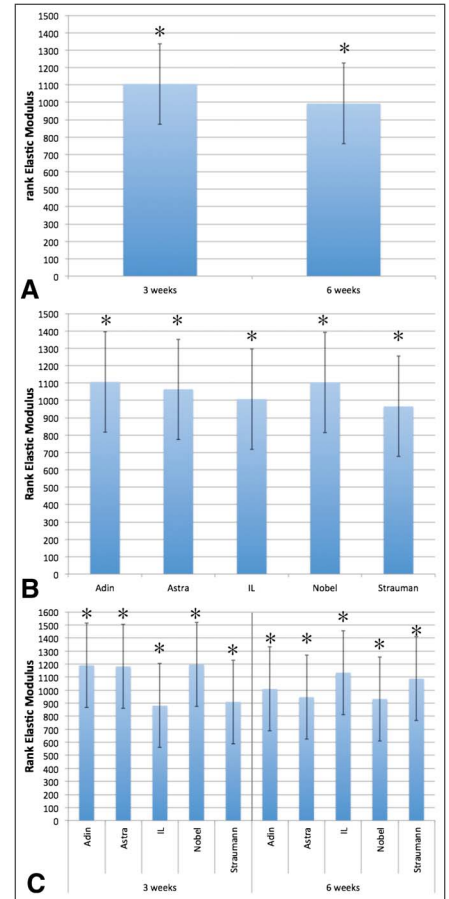
affected the amount of bone contacting implant surfaces (Fig. 4). A strong time effect was observed between 1 week and 3 weeks ($P < 0.001$), and no significant increases occurred between 3 and 6 weeks *in vivo* ($P > 0.46$) (Fig. 4). These significant increase in BIC from 1 week to 3 weeks occurred irrespective of the implant group, and no significant increase in BIC was observed from 3 to 6 weeks *in vivo* for the different implant groups. Direct comparison of BIC at 1 week showed that the IL Ossean implant presented significantly higher values than Nobel Active, Astra OsseoSpeed, and Adin OsseoFix. The Straumann SLA implant presented intermediate BIC values (lower than IL Ossean, higher than other groups, and no significant differences between them). No differences in BIC were observed between the implant groups at 3 and 6 weeks (Fig. 4).
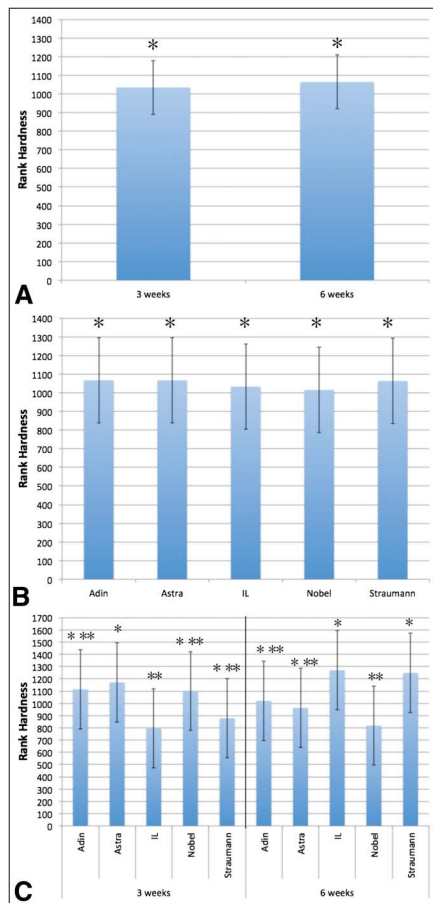
Fig. 6. Rank hardness as a function of (**A**) time, (**B**) implant system, and (**C**) time and implant system. Note that the number of asterisks depicts statistically homogeneous groups.

Bone Nanomechanical Testing

Becasue of the data inhomogeneity and substantial normality deviation usually encountered when nanoindenting heterogeneous microstructures such as bone, the data were ranked for statistical analysis. The hardness values range observed was from 0.01 to 0.362 GPa. For elastic modulus, the values ranged from just below 1 to as high as 15 GPa. The bone rank elastic modulus (E) and rank hardness (H) as a function of time $in vivo$, implant system, and time $in vivo$ and implant system are presented in Figures 5 and 6, respectively. For both parameters, time $in vivo$ (E: $P > 0.80$; H: $P > 0.75$) and implant system (E: $P > 0.90$; H: $P > 0.85$) did not significantly affect bone properties (Figs. 5 and 6). When rank elastic modulus was evaluated as a function of time $in vivo$, no significant differences were observed between the implant systems at both

times $in vivo$, and no significant differences occurred between 3 and 6 weeks for each individual system (Fig. 5, C). It should be noted that, although at 3 weeks the IL Ossean and Straumann SLA presented lowest mean elastic modulus rank values relative to others, this trend was inverted at 6 weeks.

When rank hardness was evaluated as a function of time $in vivo$, at 3 weeks, a significantly higher value ($P < 0.03$) was observed between the Astra OsseoSpeed and IL Ossean, and intermediate values were observed for the other systems. At 6 weeks, the IL Ossean and Straumann SLA groups presented significantly higher values compared with the Nobel Active ($P < 0.02$), and intermediate values were observed for the other groups. Significant increases in rank hardness were observed for the IL Ossean and Straumann SLA as a function of time $in vivo$. It should be noted that, although at 3 weeks the IL Ossean and Straumann SLA presented the lowest mean rank hardness values relative to others, this trend was inverted at 6 weeks.

DISCUSSION

This study investigated the biologic response of different commercially available implants placed in the dog tibiae by means of a histomorphometry and bone nanomechanical analysis using the nanoindenter at various healing periods. All implant groups possessed different macro-, micro-, and for some, nanostructures, which resulted in unique biologic outcomes.

From the histomorphometrical analysis, the BIC presented an implant-specific healing mechanism, especially at an early healing period of 1 week after insertion, with the IL Ossean surface presenting significantly higher BIC than the OsseoFix, OsseoSpeed, and Nobel Active surfaces. However, after 3 weeks $in vivo$, and further 6 weeks, no statistical significance could be observed between all groups tested for the BIC. This trend can be explained by the fact that all implants tested were in the range of the so-called moderately rough range and present highly biocompatible and osseoconductive properties.[30] Although there

may be initial histologic or histomorphometric differences, probably because of the differences in the geometry of the implants, it is in accordance with the previously reported $in vivo$ studies that, when longer time points are considered, such initial differences tend to contract. Given the differences in surgical instrumentation, implant macrogeometry, surface topography and chemistry, and nanogeometry, it has been suggested that distinguishing the bone healing characteristics of each implant system with the commonly used methodology is a challenge.[31,32] However, because it has been proven that the bone mineralization mechanisms differ at the molecular level between different commercially available implant systems,[17,19] it is strongly suggested that the morphologically unbeheld biologic phenomenon may actually be distinct between the implant systems tested.

Thus, it was of great interest to determine whether the bone mechanical properties differ between the 5 implant groups tested, because the histomorphometric analysis did not present any statistical significance for the BIC at some of the time points evaluated. The outcomes presented that, although there were no statistical differences in elastic modulus over time, the bone hardness proved that differences between different systems tested, suggesting that, for some implant systems, bone properties are improving with the passage of time.

The elastic modulus of bone and hardness represents and is greatly influenced by the proportion of the anisotropic type I collagen fiber and the hydroxyapatite crystal composite.[33] According to the report from Ascenzi et al[34] and Ascenzi and Bonucci E,[35] the differences in elastic modulus have been speculated to be in close relation to the turnover of the bone, ie, the maturity of the individual osteons, moreover, the distribution of their types.[34,35] In general, it has been suggested that the elastic modulus correlates with hardness.[36] However, it is also a fact that this correlation is bone type and depth dependent.[37] Thus, when evaluating the newly forming bone, which was the case for this study, the hardness may have better captured the constantly active maturation process of bone than the elastic modulus as hardness

is a complex mechanical property that involves both elastic and postyield properties.[37]

Another factor that should be taken into consideration, which may have influenced the bone mechanical property, is the alignment of the hydroxyapatite crystal.[38] As Nagisa et al[39] have stated, hydroxyapatite crystals realign themselves based on the direction of the load they bear. Because the static and dynamic load-bearing properties of each implant systems are unique because of the different macrogeometric designs of the threads,[40] it is natural to speculate that the hydroxyapatite alignment differences around the implant threads may have had significant influence on the outcomes. This study model was an unloaded model; hence, there may be an argument that the bone has a viscoelastic stress relaxation effect,[41] meaning the prestress created by the static load will gradually decrease and will not remain for as long as 3 or 6 weeks. However, because the animal was free to move during the healing period, the tibia will constantly bear mechanical stress; thus, it can be speculated that the implants placed in the tibia received a certain degree of mechanical stress throughout the healing period.

Osseointegration was originally defined as the direct BIC without interposed soft tissue at the light microscopic level.[42] However, clinically, an important factor to take in to consideration is the load-bearing capability of the implant, in other words, the mineralization status of the newly formed bone. Based on this study, it can be suggested that, along with the BIC percentage, the bone mechanical properties of the contacting bone should be taken into consideration when evaluating implant systems, because the outcomes may provide improved translational relevant interpretations.

CONCLUSIONS

Macrogeometric differences in the implant design may affect osteoconductivity and osseointegration, which will influence not only the BIC but also the bone properties over time. Interpretation of the histomorphometric and the bone mechanical data suggested that implant design is a decisive factor for osseointegration especially at the early stages of osseointegration.

DISCLOSURE

The authors claim to have no financial interest, either directly or indirectly, in the products or information listed in the article.

REFERENCES

1. Hansson S, Norton M. The relation between surface roughness and interfacial shear strength for bone-anchored implants. A mathematical model. *J Biomech.* 1999; 32:829–836.

2. Halldin A, Jimbo R, Johansson CB, et al. The effect of static bone strain on implant stability and bone remodeling. *Bone.* 2011;49:783–789.

3. Coelho PG, Granato R, Marin C, et al. The effect of different implant macrogeometries and surface treatment in early biomechanical fixation: An experimental study in dogs. *J Mech Behav Biomed Mater.* 2011;4:1974–1981.

4. Wennerberg A, Albrektsson T, Ulrich H, et al. An optical three-dimensional technique for topographical descriptions of surgical implants. *J Biomed Eng.* 1992; 14:412–418.

5. Valverde GB, Jimbo R, Teixeira HS, et al. Evaluation of surface roughness as a function of multiple blasting processing variables. *Clin Oral Implants Res.* 2013;24: 238–242.

6. Albrektsson T, Wennerberg A. Oral implant surfaces: Part 1—Review focusing on topographic and chemical properties of different surfaces and in vivo responses to them. *Int J Prosthodont.* 2004;17:536–543.

7. Buser D, Broggini N, Wieland M, et al. Enhanced bone apposition to a chemically modified SLA titanium surface. *J Dent Res.* 2004;83:529–533.

8. Sul YT. Electrochemical growth behavior, surface properties, and enhanced in vivo bone response of TiO_2 nanotubes on microstructured surfaces of blasted, screw-shaped titanium implants. *Int J Nanomedicine.* 2010; 5:87–100.

9. Sul YT, Kang BS, Johansson C, et al. The roles of surface chemistry and topography in the strength and rate of osseointegration of titanium implants in bone. *J Biomed Mater Res A.* 2009;89: 942–950.

10. Hayashi M, Jimbo R, Lindh L, et al. In vitro characterization and osteoblast responses to nanostructured photocatalytic TiO_2 coated surfaces. *Acta Biomater.* 2012;8:2411–2416.

11. Sawase T, Jimbo R, Wennerberg A, et al. A novel characteristic of porous titanium oxide implants. *Clin Oral Implants Res.* 2007;18:680–685.

12. Vouros ID, Kalpidis CD, Horvath A, et al. Systematic assessment of clinical outcomes in bone-level and tissue-level endosseous dental implants. *Int J Oral Maxillofac Implants.* 2012;27:1359–1374.

13. Jimbo R, Fernandez-Rodriguez J, Sul YT, et al. Principal component analysis: A novel analysis to evaluate the characteristics of osseointegration of different implant surfaces. *Implant Dent.* 2011;20: 364–368.

14. Johansson CB, Gretzer C, Jimbo R, et al. Enhanced implant integration with hierarchically structured implants: A pilot study in rabbits. *Clin Oral Implants Res.* 2012;23:943–953.

15. Pessoa RS, Coelho PG, Muraru L, et al. Influence of implant design on the biomechanical environment of immediately placed implants: Computed tomography-based nonlinear three-dimensional finite element analysis. *Int J Oral Maxillofac Implants.* 2011;26:1279–1287.

16. Jimbo R, Coelho PG, Vandeweghe S, et al. Histological and three-dimensional evaluation of osseointegration to nanostructured calcium phosphate-coated implants. *Acta Biomater.* 2011;7:4229–4234.

17. Jimbo R, Xue Y, Hayashi M, et al. Genetic responses to nanostructured calcium-phosphate-coated implants. *J Dent Res.* 2011;90:1422–1427.

18. Omar O, Suska F, Lenneras M, et al. The influence of bone type on the gene expression in normal bone and at the bone-implant interface: Experiments in animal model. *Clin Implant Dent Relat Res.* 2011;13:146–156.

19. Omar O, Svensson S, Zoric N, et al. In vivo gene expression in response to anodically oxidized versus machined titanium implants. *J Biomed Mater Res A.* 2010;92:1552–1566.

20. Ellingsen JE, Johansson CB, Wennerberg A, et al. Improved retention and bone-tolmplant contact with fluoride-modified titanium implants. *Int J Oral Maxillofac Implants.* 2004;19:659–666.

21. Schwarz F, Herten M, Sager M, et al. Bone regeneration in dehiscence-type defects at chemically modified (SLActive) and conventional SLA titanium implants: A pilot study in dogs. *J Clin Periodontol.* 2007;34:78–86.

22. Schwarz F, Herten M, Sager M, et al. Histological and immunohistochemical analysis of initial and early osseous integration at chemically modified and conventional SLA titanium implants: Preliminary results of a pilot study in dogs. *Clin Oral Implants Res.* 2007;18: 481–488.

23. Cooper LF, Zhou Y, Takebe J, et al. Fluoride modification effects on osteoblast behavior and bone formation at TiO2 grit-blasted c.p. titanium endosseous implants. *Biomaterials*. 2006;27:926–936.

24. Xu HH, Smith DT, Jahanmir S, et al. Indentation damage and mechanical properties of human enamel and dentin. *J Dent Res.* 1998;77:472–480.

25. Wallace JM. Applications of atomic force microscopy for the assessment of nanoscale morphological and mechanical properties of bone. *Bone.* 2012;50: 420–427.

26. Oliver WC, Pharr GM. An improved technique for determining hardness and elastic-modulus using load and displacement sensing indentation experiments. *J Mater Res.* 1992;7:1564–1583.

27. Hoffler CE, Moore KE, Kozloff K, et al. Heterogeneity of bone lamellar-level elastic moduli. *Bone.* 2000;26:603–609.

28. Hoffler CE, Guo XE, Zysset PK, et al. An application of nanoindentation technique to measure bone tissue lamellae properties. *J Biomech Eng.* 2005;127: 1046–1053.

29. Oliver WC, Pharr GM. A method for interpreting the data from depth-sensing indentation instruments. *J Mater Res.* 1992;1:601–609.

30. Wennerberg A, Albrektsson T. Effects of titanium surface topography on bone integration: A systematic review. *Clin Oral Implants Res.* 2009;20:172–184.

31. Grizon F, Aguado E, Hure G, et al. Enhanced bone integration of implants with increased surface roughness: A long term study in the sheep. *J Dent.* 2002;30: 195–203.

32. Kohal RJ, Weng D, Bachle M, et al. Loaded custom-made zirconia and titanium implants show similar osseointegration: An animal experiment. *J Periodontol.* 2004;75:1262–1268.

33. Zysset PK, Guo XE, Hoffler CE, et al. Elastic modulus and hardness of cortical and trabecular bone lamellae measured by nanoindentation in the human femur. *J Biomech.* 1999;32:1005–1012.

34. Ascenzi A, Baschieri P, Benvenuti A. The bending properties of single osteons. *J Biomech.* 1990;23:763–771.

35. Ascenzi A, Bonucci E. The tensile properties of single osteons. *Anat Rec.* 1967;158:375–386.

36. Evans GP, Behiri JC, Currey JD, et al. Microhardness and Young's modulus in cortical bone exhibiting a wide range of mineral volume fractions, and in a bone analogue. *J Mater Sci Mater Med.* 1990;1:38–43.

37. Hengsberger S, Kulik A, Zysset P. Nanoindentation discriminates the elastic properties of individual human bone lamellae under dry and physiological conditions. *Bone.* 2002;30:178–184.

38. Viswanath B, Raghavan R, Gurao NP, et al. Mechanical properties of tricalcium phosphate single crystals grown by molten salt synthesis. *Acta Biomater.* 2008;4:1448–1454.

39. Nagisa N, Nakano T, Hashiguchi N, et al. Analysis of biological apatite orientation in rat mandibles. *Oral Sci Int.* 2009;7: 19–25.

40. Hansson S, Werke M. The implant thread as a retention element in cortical bone: The effect of thread size and thread profile: A finite element study. *J Biomech.* 2003;36:1247–1258.

41. Cordey J, Blumlein H, Ziegler W, et al. [Study of the behavior in the course of time of the holding power of cortical screws in vivo]. *Acta Orthop Belg.* 1976; 42:75–87.

42. Albrektsson T. Hard tissue implant interface. *Aust Dent J.* 2008;53:S34–S38.